



Outage Performance of CoMP NOMA Networks with Selective Cell and Transmit Diversity

Nam-Soo Kim^{1*}

¹*Department of Electronic Engineering, Cheongju University, Republic of Korea*

* Corresponding author's Email: nskim@cju.ac.kr

Abstract: Most of the coordinated multipoint (CoMP) transmission studies have been focused on the sum capacity. However, the increase of the sum capacity does not guarantee the individual user's required outage performance. In this paper, we consider the outage performance of non-orthogonal multiple access (NOMA) networks with CoMP transmission under multi-cell environments. We adapt the Alamouti code for CoMP transmission to improve the outage performance of a cell-edge user. Also to provide the spatial diversity gain, cell selection with maximum channel gain is adapted. Outage probabilities of users are derived in closed-form and verified through Monte Carlo simulation. It is noticed that the outage performance improves as a near user approaches a base station, however, the error floor which does not improve the performance as the transmit power increases is observed. Since the inter cell interference (ICI) from the selected cell with NOMA causes the error floor, the selected cell with orthogonal multiple access (OMA) shows better outage performance for the near user than the cell with NOMA. Furthermore, the performance is more susceptible to the distance between the base station and the near user rather than power allocation to the user. Also, the performance of the cell-edge user shows significant improvement with the combination of the Alamouti code and the cell selection compared to the cell selection only.

Keywords: CoMP system, NOMA system, Outage performance, Selective diversity, Transmit diversity.

1. Introduction

Recently, coordinated multipoint (CoMP) transmission which sends messages from more than two base stations has been focused to improve the performance of the cellular system [1-4]. The cell-edge user generally receives poor signal strength caused by the severe fading and path loss attenuation. This phenomenon can be improved by transmitting the same messages from different base stations. However, as the number of cell-edge users increases the more communication resources such as frequency, time slot, codes are required for the CoMP transmissions. Consequently, inefficient spectral usages of the conventional orthogonal multiple access (OMA) systems are expected. To overcome the inefficient spectral usages without degradation of system performance, non-orthogonal multiple access (NOMA) has been introduced to CoMP systems [5-9]. While most of the studies of CoMP NOMA

systems concentrate on the downlink analysis, uplink analysis has recently been commenced [10].

In [5], Choi et al. introduced the Alamouti code [11] into a CoMP NOMA system for improvement on sum rate with two base stations. And an opportunistic CoMP which selects the best base station among multi-cells has been proposed to NOMA systems [6], [7, 8]. The recent study expands the CoMP transmissions to all users not only to a cell-edge user, and controls the power allocation to each user to increase the sum capacity [12]. In [9], an adaptive relay-aided multiple access (RAMA) has been proposed to increase the sum capacity as well as to lessen the transmit power of the cell-edge user for uplink communication.

Most of the studies, including upper mentioned researches for CoMP transmission have been focused on the rise of the sum capacity [5, 6, 9, 12]. On the network side the sum capacity increase is important, however, on the user side the outage performance can

be a matter of primary concern. For example, a certain network structure can increase sum capacity, but can be offered the poor performance for a designated user. In a NOMA system, the inter user interference can be eliminated using successive interference cancellation (SIC), however, the inter cell interference (ICI) can't be removed. Though the outage performance of a cell-edge user can be improved by CoMP transmission, the ICI from the base stations which are participated in CoMP transmission can cause severe degradations to a near user. In some cases, even if the transmit power of the base stations increases, the near user can't be reached to the required outage performance due to the ICI. For this reason, it is important to analyse the outage performance of individual users.

Motivated by the observation of the above mentioned reasons, we modified Choi's system model which is applied to improve the sum capacity [5]. Our proposed system model includes a multi-cell environment and adapts a selected cell transmission for CoMP. We derive the outage probabilities of the near and cell-edge users analytically. The main contributions can be summarized as follows:

- Assumes a multi-cell environment with NOMA protocol, and proposes a selected CoMP NOMA system model. A selected base station which has maximum channel gain among the neighbour base stations transmits the Alamouti code for CoMP.
- The outage probabilities of the near and cell-edge users are derived in closed-form, and verified through Monte Carlo simulation.
- The effect of the interference from the selected cell is analysed, and finds there exists an error floor which does not decrease the outage probability even if the transmit power increases.
- Analyse the space diversity gain caused by the cell selection, and performance enhancement from the Alamouti code.
- Performance comparisons are made to the NOMA and OMA cell.
- The effect of the power allocation among users in the NOMA cell is analysed.

The rest of the paper is organized as follows. Section 2 presents the proposed selective CoMP NOMA system model and analyses the signal-to-interference plus noise ratio (SINR) of users. The outage probabilities of users have derived analytically in section 3. The numerical examples of the outage probabilities of the near and cell-edge

users are given, and the analytical results are verified with the simulation in section 4. Finally, this paper concludes with the future research direction in section 5.

Notation: h_{ij} denotes the channel coefficient between BS i ($i \in \{0, 1\}$) and User j ($j \in \{1, 2, 3\}$), which has complex Gaussian distribution with zero mean and variance σ_{ij} , $h_{ij} \sim CN(0, \sigma_{ij})$. The variance σ_{ij} is given by $\sigma_{ij} = d_{ij}^{-n}$, where d_{ij} is the distance between BS i and User j , and n is the propagation loss coefficient which has typically between 3 to 6 in urban area [13]. $E[\cdot]$ and $\max\{\cdot\}$ denote the statistical expectation and the maximum value, respectively. n_i is Gaussian noise, $n_i \sim N(0, N_0)$, $i \in \{1, 2, 3\}$.

For convenience, we present the list of symbols used in this paper in Table 1.

Table 1. Table of symbols

N	the number of base stations
$S_{ij}(t)$	the messages to user j ($j \in \{1, 2, 3\}$) from BS i ($i \in \{0, 1\}$) at timeslot t ($t \in \{1, 2\}$)
$S_{ij}^*(t)$	the complex conjugate of the message $S_{ij}(t)$
P_j	average power of $S_{ij}(t)$ ($i \in \{0, 1\}$, $j \in \{1, 2, 3\}$)
γ_b^a	received SINR of a at b
$P_{o,a}$	outage probability of a

2. System model

In this study, we consider downlink CoMP networks with a home base station BS0 and neighbour N base stations (BS1, ..., BS N) in Fig.1. We assume the NOMA transmit protocol is applied to every BSs. Generally, the signal strength for a cell-edge user is poor due to the fading and path attenuation. Moreover, the interferences from



Figure. 1 Multi-cell system model

$$S_0(1) = S_{01}(1) + S_{03}(1) \quad S_1(1) = S_{12}(1) + S_{13}(1)$$

$$S_0(2) = S_{01}(2) - S_{13}^*(1) \quad S_1(2) = S_{12}(2) + S_{03}^*(1)$$

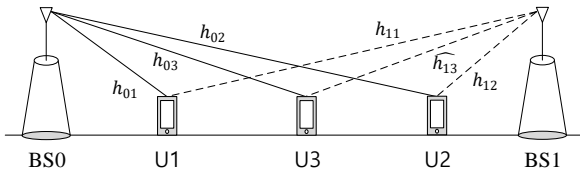


Figure. 2 CoMP system model

adjacent cells degrade the performance of the cell-edge user and causes poor spectral efficiency. To alleviate these degradations, we assume CoMP transmission for a cell-edge user.

The more base stations participated in CoMP transmissions, the better performances are expected. However, the more communication resources such as frequency, time, and codes are required. Consequently, it leads to the inefficient spectral efficiency. To enhance the spectral efficiency and the user performance, we adapt the selection of the strong BS among neighbour cells and introduce the transmit diversity of the Alamouti code.

Fig. 2 shows the simplified model of Fig.1 for easier analysis. We assume two BSs, BS0 and BS1, where BS1 denotes the selected base station among N BSs without loss of generality. Each BS has two Users, U1 and U3 for BS0 and U2 and U3 for BS1. U1 and U2 represent near users of BS0 and BS1, respectively. And U3 is the common cell-edge user of BS0 and BS1. Notice the channel coefficient between BS1 and U3 is denoted by \widehat{h}_{13} , which is the strongest channel from the selected BS, for easy distinction between channel coefficients. We assume all channels are independent Rayleigh flat fading channels. As mentioned in the introduction section, the Alamouti code is applied to increase the SINR of the cell-edge user U3 [11].

In timeslot 1, BS0 and BS1 transmit $S_0(1) = S_{01}(1) + S_{03}(1)$ and $S_1(1) = S_{12}(1) + S_{13}(1)$, respectively. In timeslot 2, BS0 and BS1 transmit $S_0(2) = S_{01}(2) - S_{13}^*(1)$ and $S_1(2) = S_{12}(2) + S_{03}^*(1)$, respectively. The average power of messages is $E[|S_{01}(1)|^2] = E[|S_{01}(2)|^2] = P_1$, $E[|S_{12}(1)|^2] = E[|S_{12}(2)|^2] = P_2$, and $E[|S_{03}(1)|^2] = E[|S_{13}(1)|^2] = P_3$. Since more power is allocated to the cell-edge user in the NOMA system, P_3 is bigger than P_1 or P_2 .

The received signal of U1 in Fig 2 can be written by

$$y_1(1) = h_{01}S_0(1) + h_{11}S_1(1) + n_1$$

$$= h_{01}\{S_{01}(1) + S_{03}(1)\} + h_{11}\{S_{12}(1) + S_{13}(1)\} + n_1$$

$$y_1(2) = h_{01}S_0(2) + h_{11}S_1(2) + n_1$$

$$= h_{01}\{S_{01}(2) - S_{13}^*(1)\} + h_{11}\{S_{12}(2) + S_{03}^*(1)\} + n_1 \quad (1)$$

Similarly, the received signal of U2 is given by

$$y_2(1) = h_{02}S_0(1) + h_{12}S_1(1) + n_2$$

$$= h_{02}\{S_{01}(1) + S_{03}(1)\} + h_{12}\{S_{12}(1) + S_{13}(1)\} + n_2$$

$$y_2(2) = h_{02}S_0(2) + h_{12}S_1(2) + n_2$$

$$= h_{02}\{S_{01}(2) - S_{13}^*(1)\} + h_{12}\{S_{12}(2) + S_{03}^*(1)\} + n_2 \quad (2)$$

The received signal of U3 is

$$y_3(1) = h_{03}S_0(1) + \widehat{h}_{13}S_1(1) + n_3$$

$$= h_{03}\{S_{01}(1) + S_{03}(1)\} + \widehat{h}_{13}\{S_{12}(1) + S_{13}(1)\} + n_3$$

$$y_3(2) = h_{03}S_0(2) + \widehat{h}_{13}S_1(2) + n_3$$

$$= h_{03}\{S_{01}(2) - S_{13}^*(1)\} + \widehat{h}_{13}\{S_{12}(2) + S_{03}^*(1)\} + n_3 \quad (3)$$

Also, the received signal of U1 after SIC can be given as

$$r_1(1) = h_{01}S_{01}(1) + h_{11}S_{12}(1) + n_1$$

$$r_1(2) = h_{01}S_{01}(2) + h_{11}S_{12}(2) + n_1 \quad (4)$$

Similarly, the received signal of U2 after SIC can be written by

$$r_2(1) = h_{02}S_{01}(1) + h_{12}S_{12}(1) + n_2$$

$$r_2(2) = h_{02}S_{01}(2) + h_{12}S_{12}(2) + n_2 \quad (5)$$

Since the Alamouti coded signals are transmitted from BS0 and BS1, the received signals are combined. The combined signals can be given as [11]

$$\begin{bmatrix} r_i(1) \\ r_i(2) \end{bmatrix} = \begin{bmatrix} h_{0i}^* & h_{1i} \\ h_{1i}^* & -h_{0i} \end{bmatrix} \begin{bmatrix} y_i(1) \\ y_i(2) \end{bmatrix} \quad (6)$$

where $i \in \{1, 2, 3\}$. While the case of $i = 3$, the channel coefficients between the selected BS1 and U3 will be denoted \widehat{h}_{13} and \widehat{h}_{13}^* instead of h_{13} and h_{13}^* , respectively, in distinction to the other channel coefficients.

The received SINR of $S_{03}(1)$ and $S_{13}(1)$ at U1 can be obtained from Eq. (6) by replacing $i = 1$,

$$\gamma_{U1}^{S_{03}(1)} = \gamma_{U1}^{S_{13}(1)} = \frac{(|h_{01}|^2 + |h_{11}|^2)^2 P_3}{ |h_{01}|^4 P_1 + |h_{01}^* h_{11}|^2 P_1 + |h_{01}^* h_{11}|^2 P_2 + |h_{11}|^4 P_2 + (|h_{01}|^2 + |h_{11}|^2) N_0 } \quad (7)$$

Assume $P_1 = P_2 = P$, then Eq. (7) becomes

$$\gamma_{U1}^{S_{03}(1)} = \gamma_{U1}^{S_{13}(1)} = \frac{(|h_{01}|^2 + |h_{11}|^2) P_3}{ (|h_{01}|^2 + |h_{11}|^2) P + N_0 } \quad (8)$$

Similarly, SINR of $S_{03}(1)$ and $S_{13}(1)$ at U2 can be obtained from Eq. (6) by replacing $i = 2$,

$$\gamma_{U2}^{S_{03}(1)} = \gamma_{U2}^{S_{13}(1)} = \frac{(|h_{02}|^2 + |h_{12}|^2)P_3}{(|h_{02}|^2 + |h_{12}|^2)P + N_0}. \quad (9)$$

After SIC, the SINR of $S_{01}(1)$ and $S_{01}(2)$ at U1 can be obtained from Eq. (4),

$$\gamma_{U1}^{S_{01}(1)} = \frac{|h_{01}|^2 P_1}{E[|h_{11}|^2]P_2 + N_0} = \gamma_{U1}^{S_{01}(2)} \quad (10)$$

From Eq. (5), the SINR of $S_{12}(1)$ and $S_{12}(2)$ at U2 after SIC is given by

$$\gamma_{U2}^{S_{12}(1)} = \frac{|h_{12}|^2 P_2}{E[|h_{02}|^2]P_1 + N_0} = \gamma_{U2}^{S_{12}(2)}. \quad (11)$$

Similarly, SINR of $S_{03}(1)$ and $S_{13}(1)$ at U3 can be obtained from Eq. (6),

$$\gamma_{U3}^{S_{03}(1)} = \gamma_{U3}^{S_{13}(1)} = \frac{(|h_{03}|^2 + |\widehat{h}_{13}|^2)P_3}{|h_{03}|^4 P_1 + |h_{03}|^2 |\widehat{h}_{13}|^2 (P_1 + P_2) + |\widehat{h}_{13}|^4 P_2 + (|h_{03}|^2 + |\widehat{h}_{13}|^2)N_0}. \quad (12)$$

Assume $P_1 = P_2 = P$, SINR of $S_{03}(1)$ and $S_{13}(1)$, γ_{U3} is given by

$$\gamma_{U3} = \frac{(|h_{03}|^2 + |\widehat{h}_{13}|^2)P_3}{(|h_{03}|^2 + |\widehat{h}_{13}|^2)P + N_0}. \quad (13)$$

3. Outage analysis

In this section, we consider the outage probability of the proposed system in Fig.2. When the received SINR bellows the predetermined threshold, the outage event occurs. The outage event of U1 happens two cases; firstly, the SINR of $S_{03}(1)$ at U1 is less than the threshold, and secondly, though the SINR of $S_{03}(1)$ at U1 is greater than the threshold, the SINR of $S_{01}(1)$ is less than the threshold. Hence, the outage probability of U1 can be written by [14-15]

$$P_{0,U1} = Pr(\gamma_{U1}^{S_{03}(1)} < \Gamma_3) + Pr(\gamma_{U1}^{S_{03}(1)} \geq \Gamma_3, \gamma_{U1}^{S_{01}(1)} < \Gamma_1) \quad (14)$$

where Γ_1 and Γ_3 are the thresholds of U1 and U3, respectively, $\Gamma_1 = 2^{R_1} - 1$ and $\Gamma_3 = 2^{R_3} - 1$. R_1 and R_3 are spectral efficiency [bps/Hz] of U1 and U3, respectively. By replacing Eq. (8) into Eq. (14), the first probability of Eq. (14) can be rearranged by

$$Pr(\gamma_{U1}^{S_{03}(1)} < \Gamma_3) = Pr(|h_{01}|^2 < \phi - |h_{11}|^2, |h_{11}|^2 < \phi) = Pr(|h_{01}|^2 < \eta, |h_{11}|^2 < \phi), \Gamma_3 < \frac{P_3}{P} \quad (15)$$

where $\phi = \Gamma_3 N_0 / (P_3 - \Gamma_3 P)$ and $\eta = \phi - |h_{11}|^2$. The outage probability of $\gamma_{U1}^{S_{01}(1)}$ in the second probability of Eq. (14) can be obtained from Eq. (10),

$$Pr(\gamma_{U1}^{S_{01}(1)} < \Gamma_1) = Pr(|h_{01}|^2 < \xi) \quad (16)$$

where $\xi = \Gamma_1 N_{t1} / P_1$ and $N_{t1} = E[X_{11}]P_2 + N_0$. For the notational simplicity, we denote $|h_{11}|^2 = X_{11}$. The outage probability of Eq. (14) can be rearranged using Eqs. (15) and (16), and can be written by

$$P_{0,U1} = Pr(|h_{01}|^2 < \eta, |h_{11}|^2 < \phi) + Pr\{(|h_{01}|^2 \geq \eta, |h_{11}|^2 < \phi), |h_{01}|^2 < \xi\}. \quad (17)$$

Denote $|h_{01}|^2 = X_{01}$. Under the Rayleigh fading environment, Eq. (17) can be expressed as [14], [16]

$$P_{0,U1} = 1 - e^{-\max\left(\frac{\eta}{E[X_{01}]}, \frac{\xi}{E[X_{01}]}\right)}. \quad (18)$$

Alternatively, Eq. (18) can be expressed as

$$P_{0,U1} = \begin{cases} 1 - e^{-\frac{\eta}{E[X_{01}]}}, & \eta \geq \xi \\ 1 - e^{-\frac{\xi}{E[X_{01}]}}, & \eta < \xi \end{cases}. \quad (19)$$

From Eq. (18) and Eq. (19), we can conclude that the outage probability of U1 becomes

$$P_{0,U1} = \max\{Pr(\gamma_{U1}^{S_{01}(1)} < \Gamma_1), Pr(\gamma_{U1}^{S_{03}(1)} < \Gamma_3)\} \quad (20)$$

where $Pr(\gamma_{U1}^{S_{01}(1)} < \Gamma_1)$ equals $1 - e^{-\xi/E[X_{01}]}$ from Eq. (9). And $Pr(\gamma_{U1}^{S_{03}(1)} < \Gamma_3)$ has two random variables as shown in Eq. (15), it can be written by

$$Pr(\gamma_{U1}^{S_{03}(1)} < \Gamma_3) = \frac{1}{E[X_{11}]} \int_0^\phi \{-e^{-(\phi-x)/E[X_{01}]}\} e^{-x/E[X_{11}]} dx, \quad \Gamma_3 < \frac{P_3}{P} \quad (21)$$

After rearrangement, we have Eq. (22) at the middle of the next page.

Similar to the outage probability of U1, the outage probability of U2 can be written by

$$P_{0,U2} = Pr(\gamma_{U2}^{S_{13}(1)} < \Gamma_3) + Pr(\gamma_{U2}^{S_{13}(1)} \geq \Gamma_3, \gamma_{U2}^{S_{12}(1)} < \Gamma_2) \quad (23)$$

Also Eq. (23) can be arranged similar to Eq. (20), we have

$$P_{0,U2} = \max\{Pr(\gamma_{U2}^{S_{12}(1)} < \Gamma_2), Pr(\gamma_{U2}^{S_{13}(1)} < \Gamma_3)\} \quad (24)$$

where $Pr(\gamma_{U2}^{S_{12}(1)} < \Gamma_2)$ can be obtained from Eq. (11),

$$Pr(\gamma_{U2}^{S_{12}(1)} < \Gamma_2) = 1 - e^{-\frac{\varepsilon}{E[X_{12}]}} \quad (25)$$

where $\varepsilon = \Gamma_2 N_{t2} / P_2$ and $N_{t2} = E[X_{01}]P_1 + N_0$. For simplicity, define $|h_{02}|^2 = X_{02}$, $|h_{12}|^2 = X_{12}$. By replacing $E[X_{01}]$ and $E[X_{11}]$ with $E[X_{02}]$ and $E[X_{12}]$, respectively, the probability of $Pr(\gamma_{U2}^{S_{13}(1)} < \Gamma_3)$ in Eq. (24) is given by Eq. (26).

The outage event of U3, which receives both signal from BS0 and BS1, happens when the received SINR is less than the threshold. Hence, the outage probability can be defined by

$$P_{0,U3} = Pr(\gamma_{U3}^{S_{03}(1)} < \Gamma_3) \quad (27)$$

$$Pr(\gamma_{U1}^{S_{03}(1)} < \Gamma_3) = 1 - e^{-\frac{\phi}{E[X_{11}]}} - \frac{E[X_{01}]}{E[X_{01}] - E[X_{11}]} e^{-\frac{\phi}{E[X_{01}]}} \left\{ 1 - e^{-\left(\frac{1}{E[X_{11}]} - \frac{1}{E[X_{01}]}\right)\phi} \right\}, \Gamma_3 < \frac{P_3}{P} \quad (22)$$

$$Pr(\gamma_{U2}^{S_{13}(1)} < \Gamma_3) = 1 - e^{-\frac{\phi}{E[X_{12}]}} - \frac{E[X_{02}]}{E[X_{02}] - E[X_{12}]} e^{-\frac{\phi}{E[X_{02}]}} \left\{ 1 - e^{-\left(\frac{1}{E[X_{12}]} - \frac{1}{E[X_{02}]}\right)\phi} \right\}, \Gamma_3 < \frac{P_3}{P} \quad (26)$$

$$P_{0,U3} = \sum_{i=1}^N \binom{N}{i} (-1)^{i-1} \left(1 - e^{-\frac{i\phi}{E[X_{13}]}} - \frac{iE[X_{03}]}{iE[X_{03}] - E[X_{13}]} e^{-\frac{\phi}{E[X_{03}]}} \left\{ 1 - e^{-\left(\frac{i}{E[X_{13}]} - \frac{1}{E[X_{03}]}\right)\phi} \right\} \right), \Gamma_3 < \frac{P_3}{P} \quad (31)$$

(pdf) of \widehat{X}_{13} . Since the selected BS1 has the maximum channel gain between BS j and U3 ($j = 1, 2, \dots, N$), the pdf in Rayleigh fading channel is given by

$$f_{X_{13}}(x) = \frac{N}{E[X_{13}]} \left[1 - e^{-\frac{x}{E[X_{13}]}} \right]^{N-1} e^{-\frac{x}{E[X_{13}]}} \\ = \sum_{i=1}^N \binom{N}{i} (-1)^{i-1} \frac{i}{E[X_{13}]} e^{-ix/E[X_{13}]}, \Gamma_3 < \frac{P_3}{P} \quad (30)$$

where the second equality holds from the binomial expansion [17]. Replacing Eq. (30) into Eq. (29), the outage probability of U3 can be obtained in Eq. (31).

As a special case, if the number of neighbour BSs is single (i.e., $i = 1$) and $E[X_{03}] = E[\widehat{X}_{13}]$, the outage probability of U3 can be obtained from Eqs. (29) and (30),

$$P_{0,U3} = \sum_{i=1}^N \binom{N}{i} (-1)^{i-1} \left(1 - e^{-\frac{i\phi}{E[X_{13}]}} - \frac{\phi}{E[X_{13}]} e^{-\frac{\phi}{E[X_{03}]}} \right), \\ \Gamma_3 < \frac{P_3}{P}, i = 1, E[X_{03}] = E[\widehat{X}_{13}]. \quad (32)$$

In the case of $P_1 = P_2 = P$, the outage probability can be rearranged from Eq. (13)

$$Pr(\gamma_{U3} < \Gamma_3) = Pr\{|h_{03}|^2 < \phi - |\widehat{h}_{13}|^2, |\widehat{h}_{13}|^2 < \phi\}, \\ \Gamma_3 < \frac{P_3}{P} \quad (28)$$

Define $|h_{03}|^2 = X_{03}$ and $|\widehat{h}_{13}|^2 = \widehat{X}_{13}$, then Eq. (28) becomes

$$Pr(\gamma_{U3} < \Gamma_3) = \int_0^\phi \left[1 - \exp\left\{-\left(\frac{\phi-x}{E[X_{03}]}\right)\right\} \right] f_{\widehat{X}_{13}}(x) dx, \\ \Gamma_3 < \frac{P_3}{P} \quad (29)$$

where $f_{\widehat{X}_{13}}(x)$ is the probability density function

4. Numerical examples

This section considers the numerical examples of the outage performance of U1 and U3. We assumed the distances between BS0 and U1 and between BS1 and U3 are assumed identical (i.e., $d_{01} = d_{12}$). The distances are normalized to the distance between BS0 and U3. Also, we assumed the transmit powers to U3 from BS0 and BS1 are identical. From this assumption, the outage probabilities of U1 and U2 are the same. Hence, we focus on the outage performance of the U1 and U3.

Fig. 3 shows the outage probability of U1 ($P_{0,U1}$), “*” denotes the results of Monte Carlo simulation, which is obtained from 1×10^8 iterations. It shows that the results from the analysis show a perfect match for the simulation. As we expected, the outage probability degrades as the distance between BS0 and U1 increases. Also, it shows the error floor - the outage does not decrease according to the increase of the transmit SNR. When $d_{01} = 0.2$ and $d_{01} = 0.3$, the outage probability of 1×10^{-3} can't be reached.

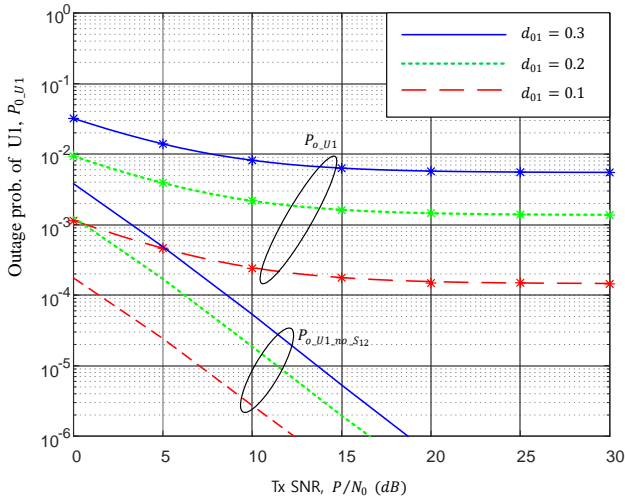


Figure. 3 Outage probability of U1 ($R_1 = R_3 = 1$, $n = 3, P_1 = P_2 = P, P_3 = 4P$)

This is because of the interference, the message of U2, from BS1. Though the inter user interference from BS0 can be cancelled by SIC, the interference from BS1 which is the inter cell interference (ICI) can't be cancelled.

$P_{o,U1,no,S12}$ in Fig. 3 means the outage probability of U1 when BS1 is OMA cell. In that case, BS1 does not transmit the messages for U2; BS1 transmits $S_1(1) = S_{13}(1)$, $S_1(2) = S_{03}^*(1)$. There is no interference from BS1, hence the error floor does not exist; the outage probability decreases as the transmit SNR increases. From this observation, we can conclude that the OMA cell which transmits a message for U3 only is preferred for the performance improvement of U1.

The outage probability of U3 for different numbers of neighbour cells is shown in Fig. 4, the results from the analysis and simulations are well matched. If the outage probability of 1×10^{-3} is required, the transmit SNR is 8.72 dB, 3.43 dB, and 0.78 dB is necessary with $N = 1, 2$, and 3, respectively. When $N = 1$ which is the system model of Choi [5], it shows the worst performance. As the number of N increases, the required transmit SNR to maintain the required outage probability decreases due to the space diversity gain. Therefore the cell selection in this paper is effective to reduce the outage probability. As a reference, the outage probability without the Alamouti code ($P_{o,U3,no_AL}$) is shown also in this figure, it reveals higher outage performance than with the code.

The outage probabilities of U1 and U3 with limited transmit power of a base station is shown in Fig. 5. The outage probability of U1 ($P_{o,U1}$) improves with the decrease of the distance between BS0 and

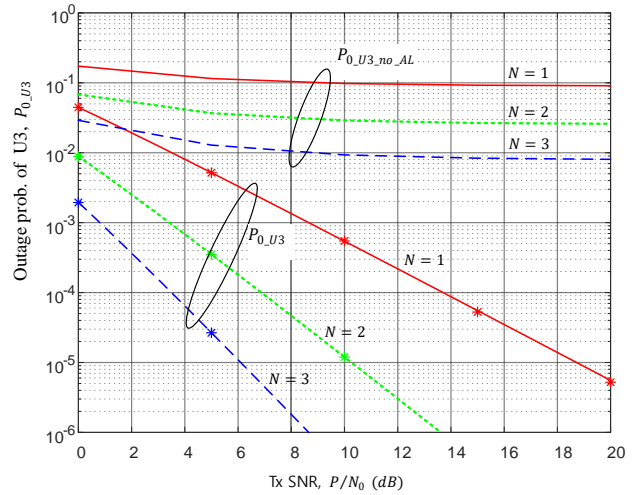


Figure. 4 Outage probability of U3 for different N ($R_3 = 1, n = 3, d_{01} = 0.1, P_1 = P_2 = P, P_3 = 4P$)

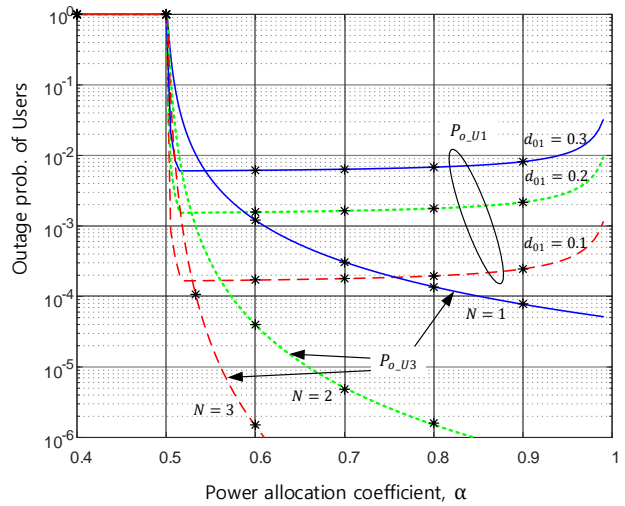


Figure. 5 Outage probability of U1 and U3 with limited transmit power ($R_1 = R_3 = 1, n = 3$, $P_T = (1 - \alpha)P_1 + \alpha P_3, P_1 = P_2, P_T/N_0 = 20$ dB)

U1. The minimum outage performance is noticed at 0.51 of power allocation coefficient α . While above 0.9 of α , the power allocation to U1 decreases and the interference from BS1 consists. Hence SINR of U1 decreases, consequently, increase the outage probability.

Notice that the outage probability of the U3 is not a function of distance as shown in Eq. (31) and Eq. (32), it is why the distance is normalized to itself. We observed that the outage probability decreases as the number of the neighbour cells and power allocation increases.

4. Conclusions

In this paper, we consider selective CoMP NOMA systems in multi-cell environment. In the proposed system, we adapt the Alamouti code for

cell-edge user and cell selection with maximum channel gain. The outage probability is derived in closed-form and the results are verified with Monte Carlo simulation. For the simulation, 1×10^8 iterations are performed.

From the analysis, we noticed that the error floor of the near user due to ICI from the selected cell happens. This phenomenon can be removed from the selected cell with OMA which has no ICI to near user. On the while, the outage performance of the cell-edge user significantly improves with the combination of the Alamouti code and the selected cell which provides the spatial diversity gain. However, only the selected cell without the Alamouti code, it is noticed that the error floor still exists and the performance improvement is not significant.

The outage probability of the near user is a function of the distance from the home base station and power allocation, it is more susceptible to the distance than the power allocation coefficient between 0.51 and 0.9. However, the performance of the cell-edge user improves with the power allocation. Further research will be focused on the improved network structure which enhances both the sum rate and outage performance of users in CoMP NOMA system.

Conflicts of Interest

The authors declare no conflict of interest.

References

- [1] M. K. Karakayali, G. J. Foschini, and R. A. Valenzuela, "Network Coordination for Spectrally Efficient Communications in Cellular Systems", *IEEE Wireless Communications*, Vol. 13, No. 4, pp. 56-61, 2006.
- [2] M. Sawahashi, Y. Kishiyama, A. Morimoto, D. Nishikawa, and M. Tanno, "Coordinated Multipoint Transmission/reception Techniques for LTE-advanced," *IEEE Wireless Communications*, Vol. 17, No. 3, pp.26-34, 2010.
- [3] S. Brueck, L. Zhao, J. Giese, and M. A. Amin, "Centralized Scheduling for Joint Transmission Coordinated Multi-point in LTE-advanced", In: *Proc. of International ITG Workshop on Smart Antennas (WSA)*, Bremen, Germany, pp. 177-184, 2010.
- [4] D. Lee, H. Seo, B. Clerckx, E. Hardouin, D. Mazzarese, S. Nagata, and K. Sayana, "Coordinated Multipoint Transmission and Reception in LTE-advanced: Deployment Scenarios an Operational Challenges", *IEEE Communications Magazine*, Vol. 50, No. 2, pp.148-155, 2012.
- [5] J. Choi, "Non-orthogonal Multiple Access in Downlink Coordinated Two-point Systems", *IEEE Communications Letters*, Vol. 18, No. 2, pp. 313-316, 2014.
- [6] Y. Tian, S. Lu, A. Nix, and M. Beach, "A Novel Opportunistic NOMA in Downlink Coordinated Multi-point Networks", In: *Proc. of Vehicular Technology Conference (VTC2015-Fall)*, Boston, USA, 2015. doi: 10.1109/VTCFall.2015.7390804
- [7] Y. Tian, A. R. Nix, and M. Beach, "On the Performance of Opportunistic NOMA in Downlink CoMP Networks". *IEEE Communications Letters*, Vol. 20, No. 5, pp. 998-1001, 2016.
- [8] Y. Tian, A. Nix, and M. Beach, "On the Performance of Multi-tier NOMA Strategy in Coordinated Multi-point Networks", *IEEE Communications Letters*, Vol. 21, No. 11, pp. 2448-2451, 2017.
- [9] Q. Zhou, Y. Ma, L. Bai, J. Choi, and Y.-C. Liang, "Relay-aided Multiple Access Scheme in Two-Point Joint Transmission", *IEEE Transactions on Vehicular Technology*, Vol. 68, No. 6, pp. 5629-5641, 2019.
- [10] Y. Sun, Z. Ding, X. Dai, and O. A. Dobre, "On the Performance of Network NOMA in Uplink CoMP System: a Stochastic Geometry Approach", *IEEE Transactions on Communications*, Vol. 867, No. 7, pp. 5084-5098, 2019.
- [11] S. M. Alamouti, "A Simple Transmit Diversity Technique for Wireless Communications", *IEEE Journal on Selected Areas in Communications*, Vol. 16, No. 8, pp. 1451-1458, 1998.
- [12] Z. Liu, G. Kang, L. Lei, N. Zhang, and S. Zhang, "Power Allocation for Energy Efficiency Maximization in Downlink CoMP Systems with NOMA", In: *Proc. of IEEE Wireless Communications and Networking Conference (WCNC)*, San Francisco, USA, pp.1-6, 2017.
- [13] A. Goldsmith, *Wireless Communications*, Cambridge University Press, New York, 2005.

- [14] Y. Liu, Z. Ding, M. ElKashlan, and H. V. Poor, “Cooperative Non-orthogonal Multiple Access in 5G Systems with SWIPT”, In: *Proc. of the 23rd European Signal Processing Conf. (EUSIPCO)*, Nice, France, pp. 1999-2003, 2015.
- [15] N.-S. Kim, “Overlay Cognitive Radio NOMA Networks with Selected Relay and Direct link”, *International Journal of Intelligent Engineering and Systems*, Vol. 13, No. 1, pp. 181-190, 2020.
- [16] N.-S. Kim, “Cooperative Overlay Cognitive Radio NOMA Network with Channel Errors and Imperfect SIC”, *International Journal of Intelligent Engineering and Systems*, Vol. 12, No. 5, pp. 224-231, 2019.
- [17] K. Tourki, H.-C. Yang, and M. –S. Alouini, “Accurate Outage Analysis of Incremental Decode-and-forward Opportunistic Relaying”, *IEEE Transactions on Wireless Communications*, Vol. 10, No. 4, pp. 1021-1025, 2011.